Aryldiazonium reduction mechanism deciphered by scanning electrochemical microscopy through an EC' process

Nikolaos Kostopoulos, Viacheslav Shkirskiy, Catherine Combellas, Frédéric Kanoufi, Tony Breton, Jean-Marc Noël

Aryldiazonium reduction mechanism deciphered by scanning electrochemical microscopy through an EC' process.

Nikolaos Kostopoulos,[a] Viacheslav Shkirskiy,[a] Catherine Combellas,[a] Frédéric Kanoufi,[a] Tony Breton,[b] Jean-Marc Noël[a]*

[a] Université Paris Cité, ITODYS, CNRS, F-75013, Paris, France

[b] Univ Angers, CNRS, MOLTECH-Anjou, SFR MATRIX, F-49000 Angers, France.

Corresponding author: Noël, Jean-Marc (jean-marc.noel@cnrs.fr)

Highlights

- Scanning electrochemical microscope (SECM) to investigate the redox cross reduction of 4-nitrobenzenediazonium.
- SECM combined with numerical simulations to describe and quantify the whole EC' mechanism.
- Identification of a side reaction involving the reactive aryl radical species.

Abstract

Homogeneous redox catalysis, often associated to EC' mechanisms, is an elegant way to investigate electron transfer processes. Among the electrochemical tools employed to decipher such processes, scanning electrochemical microscopy (SECM) is a powerful technique to unravel complex EC' mechanisms, especially those involving short life time intermediates. Herein, it is employed to decipher the mediated reduction of 4-nitrobenzenediazonium by the reduced form of a redox mediator, chloranil, electrogenerated at the tip of the SECM. This strategy that

relocates the reduction of the aryldiazonium far from the tip surface allows protecting the tip from passivation and producing very reactive intermediates, *i.e.* aryl radicals, in solution. Combined with simulations, the SECM in the feedback mode allows describing the whole reduction mechanism and evidences the reaction pathway implying reactive radical species issued from the aryldiazonium reduction. Particularly, it is demonstrated that an irreversible reaction occurring between the aryl radical and the redox mediator is a predominant side reaction.

Keywords

- Scanning electrochemical microscopy

- EC' mechanism

- Aryldiazonium

- Electroreduction

- Reactive intermediate species

Introduction

The electrocatalytic regenerative mechanism usually known as the EC' mechanism[1] involves a reversible redox compound A, that is reduced (or oxidized) into B at the electrode via a heterogeneous electron transfer "E" (equation (1)). It is followed by a homogeneous catalytic chemical reaction in solution where B is regenerated back to A by reacting with another species, X, present in solution during the chemical reaction "C" (equation (2)).

"E" **A** + e^- ⇌ B (1)

"C" B + X ⇌ **A** + Y (2)

The EC' mechanism then allows mediating the reduction (or oxidation) of X in solution through the reversible redox mediator couple A/B. This mechanism is at the basis of many electrocatalytic processes including redox catalysis,[2,3] enzymatic electron transfer using redox mediators,[4-7] electrochemiluminescence[8] or sensors.[9-11] Such processes are characterized by an increase of the current recorded at the electrode for the electrochemical conversion of A to B due to the continuous regeneration of the passive form, A, of the redox species in solution and of its active form, B, at the electrode. This characteristic electrochemical signature can be exploited to quantitatively evaluate the mechanism of the redox mediated transformation of the species X, usually by cyclic voltammetry[12,13] or chronoamperometry.[14] Alternatively, scanning electrochemical microscopy (SECM) is also a very useful technique to study such electrochemical processes.[9, 15-17] Even if the current increase recorded at the ultramicroelectrode (UME, used as the tip of the SECM) can provide a quantitative description of EC' processes similarly to the classical electrochemical tools, the analysis of the perturbation of this current due to the confinement offered by the SECM configuration can bring insightful information.[18-20] For instance, usually combined with numerical simulations, this strategy allowed deciphering complex EC' reactions implying reactive intermediates species such as those involved in electrochemiluminescence, ECL,[19 20] or the Belousov-Zhabotinsky reaction.[18] SECM also offers an elegant approach to

deliberately trigger EC' processes in order to capture, quantify, and characterize reactive intermediates formed homogeneously such as H_2O_2,[21] or HO•,[22] and also adsorbed intermediate species generated during heterogeneous photoelectrochemical [23, 24] or electrocatalytic processes.[25-27]

In the present work, SECM is employed to investigate the 4-nitrobenzenediazonium (4-NBD) reduction mechanism through a mediated reduction following an EC' mechanism illustrated in Figure 1a. The aryldiazonium reduction strategy allows for a covalent attachment of a broad range of chemical moieties to a wide range of surfaces. However, it suffers from poor control of the deposited layer's thickness and structure due to an uncontrolled electrogeneration of highly reactive aryl radicals from the diazonium[28-31] electroreduction, which impedes the fine tuning of an organized film.[32, 33] Among the strategies employed to control the film thickness,[34-38] the one based on an EC' mechanism, namely the redox cross-reaction, was developed.[29] Briefly, it consists of the redox mediated reduction of the aryldiazonium, which relocates rapidly the reduction of the aryldiazonium in the diffusion layer of the electrode. Therefore, it prevents at the early stage the grafting of the reactive aryl radical species issuing from the aryldiazonium reduction.[29, 39-41] Very recently, this mediated reduction strategy was exploited to evidence the formation of the highly reactive diazenyl species as a preliminary intermediate, suggesting that the 4-nitrobezenediazonium reduction yields the nitroaryl radical in a stepwise electron transfer followed by C-N bond breaking.[38] Herein, this system is investigated by SECM in feedback mode operated at an unbiased substrate (illustrated in Figure 1a). It is combined with numerical simulations to unravel this

reduction mechanism and investigate the role of the reactive intermediate species involved in the process.

Material and methods

Chemicals

All reagents and solvents were purchased from Acros Organics or Sigma Aldrich. Chloranil, 4-nitrobenzenediazonium (NBD) tetrafluoroborate, tetrabutylammonium hexafluorophosphate ($TBAPF_6$, supporting electrolyte), N,N-dimethylformamide (DMF, anhydrous, 99.8%) were used as received, without further purification.

Scanning electrochemical microscopy (SECM) experiments

Electrochemical measurements were performed using a bipotentiostat (Electrochemical Analyzer) from CH Instruments (Model #760C, IJCambria, UK). Ultramicroelectrode positioning and SECM movements were handled via a Newport Universal Motion Controller/Driver, model ESP300 (Newport Corporation, Irvine, California) operated through a homemade program using LabView. Ultramicroelectrodes (UMEs) with $R_G = 10$ were fabricated using 1.0 mm/0.5 mm (inner diameter/outer diameter) borosilicate glass capillaries from Sutter Instruments (Novato, California, USA), 25 µm diameter gold wire (99.99%, Goodfellow Cambridge Ltd., Huntingdon, UK), and a laser puller from Sutter instruments (Model# P-2000). A Pt wire was used as counter electrode, and a silver wire coated by AgCl as the reference electrode.

The SECM approach curves represent the normalized current $I = i/i_{,inf}$ as a function of the normalized distance. L = d/a; d is the separation distance between the UME and

the substrate, a the radius of the conductive part of the UME. They were recorded using either a glass slide as insulating substrate or at a 3mm glassy carbon electrode carefully polished before each experiment with a 1 µm alumina paste, sonicated in an ethanol bath and then washed with ethanol. All the experiments were performed at an approach rate of 1 µm.s^{-1} under air since O_2 reduction does not interfere at the potentials used.

Simulations

All numerical simulations were performed using the transport of diluted species module on COMSOL Multiphysics v5.6. The UME and substrate geometry were simulated using a 2D axis-symmetric domain as presented in Figure S1 of the Supplementary Material (SM). The UME dimension (a) and the ratio between the UME radius and the radius of the metal center (R_G) were determined respectively from the initial diameter of the wire inserted in the capillary and from the negative feedback approach curves. Besides all the used parameters are shown in Table S1 in SM. Among them, the diffusion coefficient of chloranil (D_{ch} ~ 7x10^{-6} $cm^2.s^{-1}$) was estimated from the UME steady state current using equation 3.

$$i_{inf} = 4nFD_{ch}C_{ch}a \qquad (3)$$

where i_{inf} is the current measured in the bulk solution, F is the faradaic constant, n the number of electrons of the reaction, a the radius of the electrode and C_{ch} is the concentration of chloranil.

The simulated approach curves were solved using the UME-substrate distance as a parameter varying from 0.1 to 80 µm with 1 µm steps (simulations were performed

in transient mode, each new UME-substrate distance was computed for 100s). The simulated current value was extracted at t = 100 s for each step to ensure the steady state conditions.

Results and discussion

Description of the experimental SECM approach curves

The SECM approach curves were first recorded with 2 mM of chloranil either towards a glass substrate or an unbiased glassy carbon (GC) one using a 25 µm diameter gold UME as the SECM tip. As shown in Figure 1b the former curve presents pure negative feedback that fits with the analytical expression given for $R_G = 10$.[42] On the other hand, the approach curve of the GC substrate presents a classical positive feedback[42,43] that can be fitted considering a re-oxidation of the radical anion of chloranil at the GC substrate with a heterogeneous rate constant of chloranil $k_{s,GC} = 3 \pm 0.5 \times 10^{-2}$ cm.s^{-1}. This value extracted from multiple approach curves (Figure S2 in SM) was further considered for all the simulations in this work.

As depicted in Figure 1a, when adding 4-NBD, one expects the reduced form of the redox probe (*i.e.* the radical anion of chloranil) to reduce 4-NBD, regenerating chloranil via an EC' type reaction. After addition of 2 mM of 4-NBD, the approach curve performed at the glass substrate presents pure negative feedback similar to the one recorded without aryldiazonium in solution (Figure S3 in SM). The approach curve recorded at the GC substrate results in a very different shape that can be decomposed in two regions depending on the normalized UME-substrate distance, L. First, starting from large L values, a decrease of the current occurs until the UME reaches a normalized distance L ~ 1. Then for shorter distances, the current increases

until the UME touches the surface (current inflection). As shown in Figure S4 in SM, two successive approach curves present the exact same shape, attesting that at the time scale of the experiment, the possible grafting of the aryl radical formed during the process remains insufficient to passivate the glassy carbon substrate and the Au UME. Analogous feedback response was reported in the literature for different mechanistic investigations by SECM, all implying the redox mediator into a competing follow-up chemical reaction. This situation was particularly observed for EC' mechanisms as in redox catalysis or ECL processes.[19,44] To further investigate quantitatively the origin of this feedback response, numerical simulations were performed.

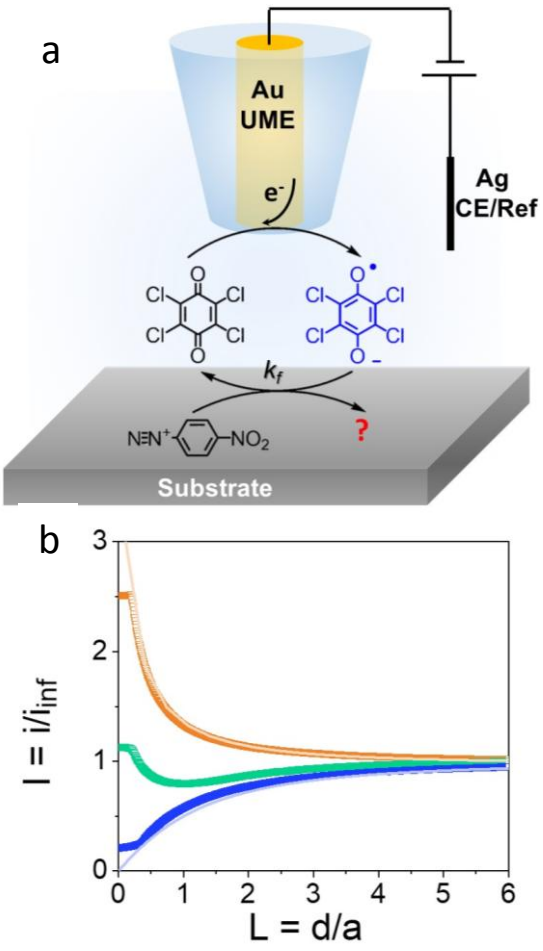

Figure 1: a) SECM configuration to investigate the mediated reduction of 4-nitrobenzene diazonium. b) Approach curves recorded with 2 mM of chloranil at a glass substrate (□) or at an unbiased 3 mm diameter glassy carbon substrate (□) without and (□) after addition of 2 mM of 4-nitrobenzenediazonium. All the experiments were performed in DMF solutions in the presence of 0.1 M $TBAPF_6$, applying -0.3 V vs Ag pseudo reference at a 25 µm diameter gold UME at 1 µm.s^{-1}. Lines are the simulated curves for pure positive (—) and negative feedback (—) considering the heterogeneous electron transfer rate for the chloranil at the unbiased GC electrode $k_{sc,GC}$ = 3x10^{-2} cm.s^{-1} and RG = 10.

Catalytic EC' mechanism

The diazonium reduction leads to the breaking of the C-N_2 bond. Since the nature of this bond breaking step, as being either concerted or subsequent to the electron transfer (stepwise), is still a debate, we have simulated both situations as illustrated in Figure 2a and b.

Let's first consider a stepwise mechanism. In this process, the current recorded at the UME depends on i) the rate of the homogeneous electron exchange between the reduced form of chloranil and the aryldiazonium (k_f) yielding the diazenyl radical and ii) the further dissociation of the latter to form the aryl radical (k_d). Noteworthy, it is assumed that the reduction of the aryldiazonium by the reduced form of chloranil stops at the aryl radical step since further reduction of the aryl radical into its corresponding anion occurs at a potential at least 0.5 V more negative than the redox potential of chloranil.[45, 46] As explained in Figure S5 in SM, the influence of both k_f and k_d was investigated by looking at the current drop in the simulated

approach curves. The 3D diagram shown in Figure S5 in SM evidences that the current drop is strongly affected by variations in k_f: the higher k_f and the more pronounced the current drop, meaning that the approach curve departs more from the substrate kinetics feedback limit (upper approach curve in Figure 2a). The influence of k_f on the approach curve is mainly within the 10^3 $M^{-1}.s^{-1} < k_f < 10^6$ $M^{-1}.s^{-1}$ range. Similar trends are observed for k_d: the higher k_d the more the approach curve departs from the substrate kinetics limits. However, under the chosen configuration, the maximum effect is observed for $k_d = 10^3$ s^{-1}. This means that for intermediates having lifetime $\tau < 1$ ms ($1/k_d$) the SECM approach curves are only kinetically governed by the mediated electron transfer step k_f. Since k_d values, reported in the literature, are at least one order of magnitude higher than this limit,[38, 47, 48] in such an experimental configuration it is impossible to evaluate the value of kd and therefore differentiate between a stepwise or a concerted bond breaking. Noteworthy, the evaluation of k_d would require smaller UME and the choice of the appropriate UME should be selected based on the dimensionless parameter of the dissociation step $k_d a^2/D$ with *a* the radius of the UME and D the diffusion coefficient of the redox mediator.

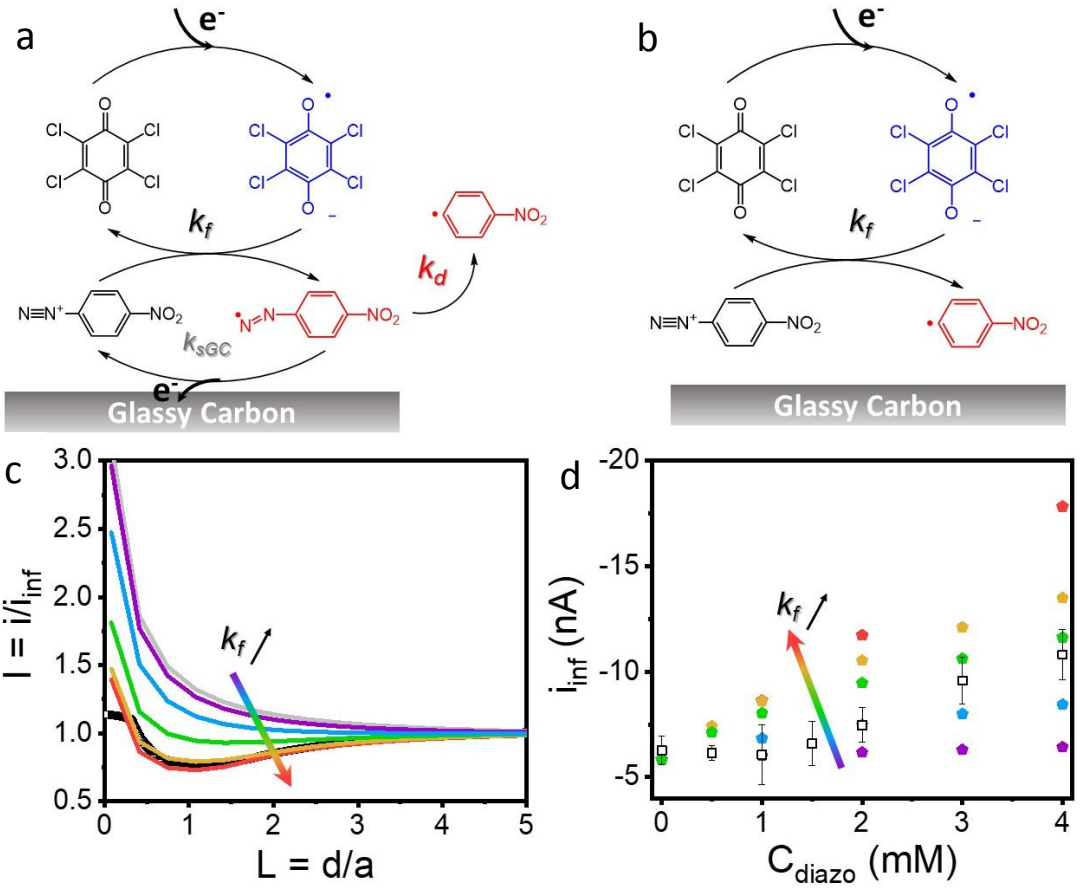

Figure 2: a) Stepwise or (b) concerted mechanisms envisaged for the mediated reduction of 4-nitrophenyldiazonium. c) Normalized experimental approach curve (□) and simulated ones for a classical feedback behavior (—) and for $k_f = 10^2$ (—), 10^3 (—), 10^4 (—), 10^5 (—), 10^8 (—) $M^{-1}.s^{-1}$. d) Average infinite distance current, i_{inf}, determined experimentally (□) at a distance between the UME and the substrate d ≥ 100 µm based on N ≥ 5 i_{inf} values for various 4-NBD concentrations, C_{diazo}, compared to simulated values for $k_f = 10^2$ (⬟), 10^3 (⬟), $5x10^3$ (⬟), 10^4 (⬟), 10^6 (⬟) $M^{-1}.s^{-1}$.

In the case of high k_d values (or also for the concerted mechanism) the process is only controlled by the reaction rate constant k_f. Its effect on the approach curve shape is depicted in Figure 2c. For $k_f < 10^2$ $M^{-1}.s^{-1}$, all simulated approach curves display the classical positive feedback behavior showing that its effect can be

neglected. However, while increasing k_f value up to 10^8 $M^{-1}.s^{-1}$, the shape of the simulated approach curves deviates from the classical positive feedback behavior and a current drop similar to the one observed experimentally is observed. The experimental approach curve fit is obtained for 10^5 $M^{-1}.s^{-1} < k_f < 10^8$ $M^{-1}.s^{-1}$ in a good agreement with the value recently reported in the literature considering a concerted mechanism ($k_f = 10^6$ $M^{-1}.s^{-1}$).[49]

Further mechanistic information is provided from the absolute value (unnormalized) of the current recorded at the UME. Indeed, as recalled in the introduction, the EC' mechanism is usually characterized by an increase of the current due to the solution phase regeneration of the redox mediator. This regeneration and the current enhancement do not necessarily imply the presence of a substrate and are observed at large distances from the substrate, *i.e.* > 100 µm. As shown in the approach curves in Figure S6 in SM, even if qualitatively an increase of the infinite distance current (i_{inf}) was observed after adding 2 mM of 4-NBD, this increase is significantly lower than expected considering the values of $k_f > 10^5$ $M^{-1}.s^{-1}$ as suggested from the approach curve simulations. This is further supported by Figure 2d that represents the experimental evolution of the infinite distance current, i_{inf}, recorded at the UME (UME held at > 100 µm above the GC substrate) plotted versus the concentration of 4-NBD, C_{diazo}, added in the solution. There is a discrepancy between the experimental variations of i_{inf} with C_{diazo} and the simulated ones using $k_f = 10^6$ $M^{-1}.s^{-1}$ (red symbols in Figure 2d). The observed evolution would rather roughly correspond to electron exchange rate within $10^3 < k_f < 5x10^3$ $M^{-1}.s^{-1}$, which cannot reproduce the current drop observed experimentally (Figure 2c). This antagonism suggests that the EC' reaction mechanism is not sufficient to explain the homogeneous reduction of 4-

NBD by the reduced chloranil and likely involves secondary reactions playing a key role in the feedback loop of the redox species.

EC' mechanism considering the reactivity of the aryl radical species.

Carefully comparing the experimental evolution of i_{inf} with C_{diazo} and the simulated ones, obtained considering the classical EC' mechanism, the discrepancy between the apparent k_f value obtained either from simulations of the infinite distance UME current or approach curves suggests that the regeneration of the redox mediator is somehow slowed down at infinite distance. This phenomenon could have its origin in a lower concentration of the aryldiazonium reacting with the redox probe and/or in a lower concentration of the redox probe itself. The former hypothesis could result, as previously reported,[48] from a coupling reaction (dimer formation) between the reactive aryl radical, produced by the bond breaking step, and the diazonium counterpart.

Therefore, as a first attempt, the reaction between the aryl radical and the aryldiazonium, as shown in Figure 3a (red pathway), was implemented in the model. The effect of the rate constant k_f' of this reaction on the infinite distance UME current, i_{inf}, was investigated as a function of C_{diazo}. The results presented in Figure 3b show that an increase of k_f', while maintaining k_f at 10^6 $M^{-1}.s^{-1}$, indeed results in decreasing the infinite distance current values. However, even using k_f' value up to 10^7 $M^{-1}.s^{-1}$, the simulated current is still overestimated compared to the experimental one as soon as the aryldiazonium concentration exceeds 0.5 mM, meaning that this mechanism does not explain the infinite distance current evolution.

We then considered the possibility of a chemical reaction between the aryl radical and chloranil. Noteworthy, the same reaction can be envisaged with the reduced form of chloranil. The effect of the rate constant, k_f'', associated to this reaction was studied while maintaining $k_f' = 0$. Using a similar approach as above, the evolution of the infinite distance current for various diazonium concentrations when increasing k_f'' was investigated assuming $k_f = 10^6\ M^{-1}.s^{-1}$. The results are presented in Figure 3c. Interestingly when increasing k_f'', the whole set of experimental infinite distance currents i_{inf} values for different NBD concentrations could be reproduced by the simulations using $k_f'' \sim 10^5\ M^{-1}.s^{-1}$. This result favors a reaction between the redox species and the aryl radical during the EC' process. Noteworthy, it was already evidenced that 2,2-diphenyl-picrylhydrazyl (DPPH), used as a redox mediator, couples to aryl radicals issuing from aryldiazonium reduction, even if this coupling was initially attributed to a radical trapping mechanism at the interface.[41] Even if at this stage we don't have yet the identification of the product, we assume that a similar radical-radical reaction between the aryl radical and the chloranil radical anion occur within the reaction layer of the UME.

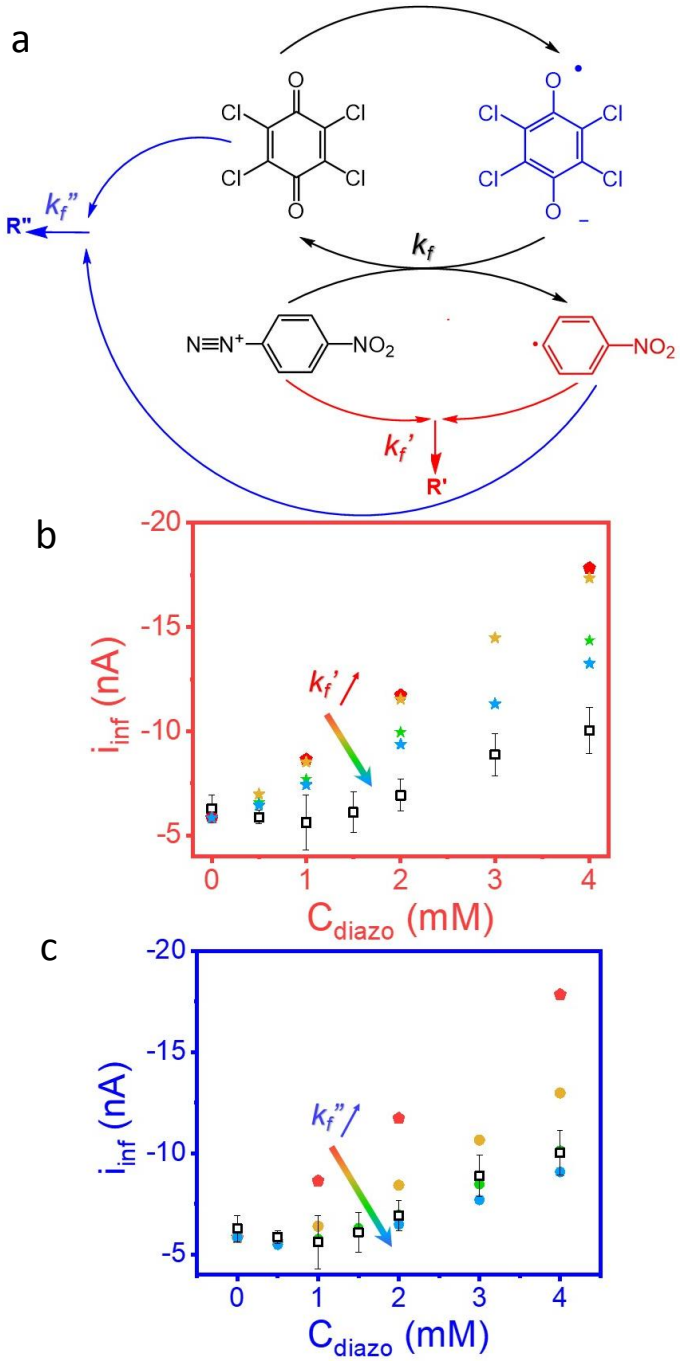

Figure 3: a) Mechanism involving the aryl radical formed during mediated reduction and 4-NBD by chloranil. b) Average infinite distance current, i_{inf}, determined experimentally (□) for various 4-NBD concentrations shown in Figure 2c compared to the simulated ones for $k_f = 10^6$ $M^{-1}.s^{-1}$ (⬟) and b) $k_f' = 10^3$ (★), 10^5 (★), 10^7 (★) $M^{-1}.s^{-1}$ and c) $k_f" = 10^4$ (★), $5x10^4$ (★), 10^5 (★)$M^{-1}.s^{-1}$.

Quantitative analysis of the whole mechanism

To summarize, the infinite distance current behavior suggests that the reduction of 4-NBD by an electrogenerated redox probe is governed by both the homogeneous electron exchange, k_f, and a chemical reaction involving the radical derived from 4-NBD, k_f". The quantitative contribution of each path was determined by reproducing the whole approach curve (the absolute current value as a function of the UME-substrate distance). By considering the values of k_f and k_f" determined separately above ($k_f = 10^6\ M^{-1}.s^{-1}$ and $k_f" = 10^5\ M^{-1}.s^{-1}$ for $C_{diazo} = 2$ mM), the current drop observed in the approach curve could not be reproduced satisfactorily. As both k_f and k_f" affect the infinite distance current and the approach curve, these rate constants should be adjusted simultaneously in a quantitative description of the mechanism. To do so, the respective effects of k_f and k_f" on the current drop, namely i_{min}, and i_{inf}, were considered simultaneously. First, a 3D diagram showing their effect on the current drop is presented in Figure 4a. This diagram reveals that an increase of k_f has a strong effect to increase the current drop, as also shown in the simulated approach curves of Figure 2c. On the contrary, an increase of k_f" leads, in a lesser extent, to a lowering of the current drop. In this diagram, the experimental current drop value averaged over 4 approach curves was added (light grey plan) that allows to highlight the possible (k_f , k_f'') couples that could fit the current drop (*i.e.* the intersection between the diagram and the light grey plane). In a second 3D diagram presented in Figure 4b, the effect of the very same rate constants on i_{inf} was studied. It is evidenced that k_f has only a slight effect on i_{inf} for $k_f < 10^5\ s^{-1}$. Contrariwise, an increase of k_f" leads to a significant decrease of i_{inf} due to the decrease of the redox regeneration at the UME. Similarly to Figure 4a, the light grey plane corresponds to

the averaged value of the experimental i_{inf}. Exploiting both diagrams, a unique couple of $k_f \sim 10^5\ M^{-1}.s^{-1}$ and $k_f'' \sim 5x10^4\ M^{-1}.s^{-1}$ (red traces in Figures 4a and b) was determined to match both i_{min} and i_{inf} values. As demonstrated in Figure 4c for 2mM of 4-NBD and in Figure S7 in SM for other concentrations, this couple of rate constants could also fit the whole experimental approach curves.

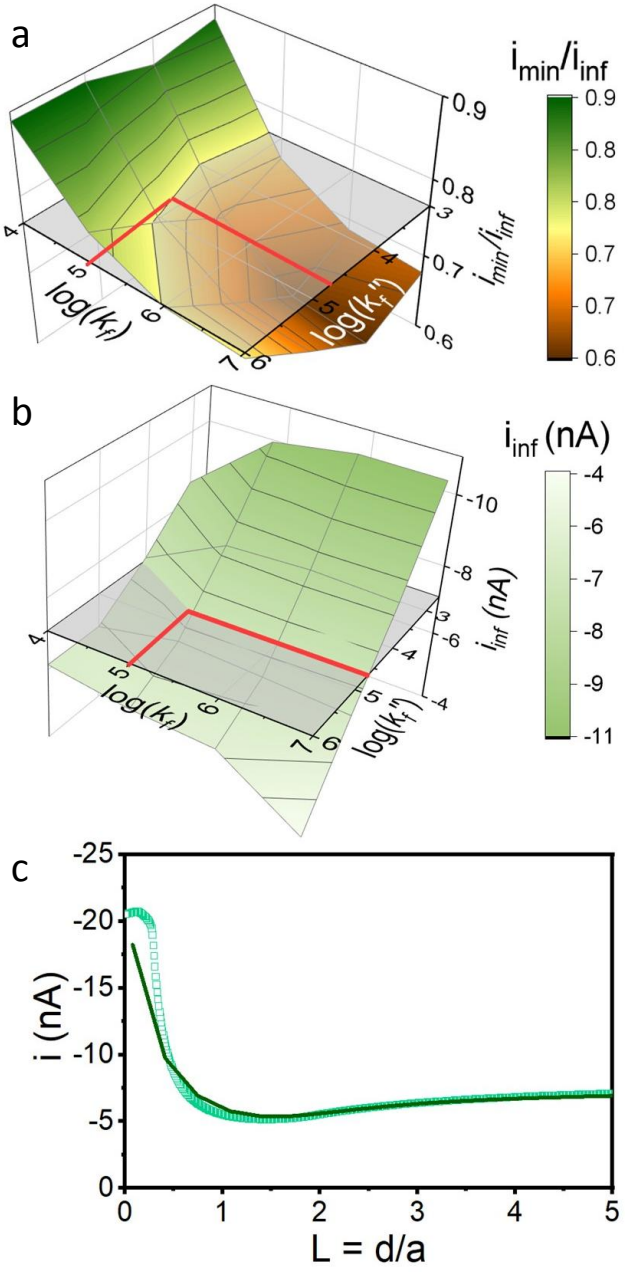

Figure 4: a, b) 3D diagrams showing the effect of k_f and k_f" on a) the normalized current drop, i_{min}/i_{inf}, of the approach curves and b) the infinite distance current, i_{inf}. c) (□) approach curve of Figure 1a compared to the simulated one using the combination of $k_f \sim 10^5\ M^{-1}.s^{-1}$ and $k_f'' \sim 5.10^4\ M^{-1}.s^{-1}$ determined from the 3D diagrams (red traces).

Conclusion

The mechanism of the mediated electrochemical reduction of 4-NBD was deciphered quantitatively by SECM in the feedback mode combined with numerical simulations. The shape of the approach curves mainly depends on the electron transfer exchange reaction between the aryldiazonium and the reduced form of the redox mediator generated at the UME. However, a simple EC' mechanism is insufficient to fully understand this mediated reduction process. It turned out that the mechanism involves a side reaction in which the reactive intermediate generated (the aryl radical) reacts predominantly with the redox mediator. The precise description of the mechanism allowed determining the reaction rate between the aryl radical and the former species. This work demonstrates that exploiting SECM approach curves in the feedback mode allows deciphering quantitatively complex mechanisms involving EC' patterns. It could be further employed to study other similar reactions. Particularly here, the EC' mechanisms triggered by SECM is a powerful strategy to quantify the coupling reactions between redox mediator and radical species that could be of high interest in the field of redox radical trapping processes.[50]

Aknowledgments

We gratefully thank the ANR JCJC program (PIRaNa project, ANR-20-CE42-0001) for the financial support.

References

1. J.-M. Savéant, in *Elements of Molecular and Biomolecular Electrochemistry*, 2006, pp. 78-181.
2. A. G. Gilicinski and D. H. Evans, *J. Electroanal. Chem. Interfacial Electrochem.*, 1989, **267**, 93-104.
3. H. Lund, K. Daasbjerg, T. Lund and S. U. Pedersen, *Acc. Chem. Res.*, 1995, **28**, 313-319.
4. R. Bourbonnais, D. Leech and M. G. Paice, *Biochimica et Biophysica Acta (BBA) - General Subjects*, 1998, **1379**, 381-390.
5. C. Moreno, C. Costa, I. Moura, J. Le Gall, M. Y. Liu, W. J. Payne, C. van Duk and J. J. G. Moura, 1993, **212**, 79-86.
6. P. N. Bartlett and K. F. E. Pratt, *J. Electroanal. Chem.*, 1995, **397**, 61-78.
7. J. Galceran, S. L. Taylor and P. N. Bartlett, *J. Electroanal. Chem.*, 2001, **506**, 65-81.
8. F. Kanoufi and A. J. Bard, *The Journal of Physical Chemistry B*, 1999, **103**, 10469-10480.
9. F. F. Silva, G. N. Meloni, A. S. Lima and M. Bertotti, *J. Electroanal. Chem.*, 2022, **919**, 116543.
10. J. M. Saveant and E. Vianello, *Electrochim. Acta*, 1965, **10**, 905-920.
11. H. R. Zafarani, K. Mathwig, E. J. R. Sudhölter and L. Rassaei, *J. Electroanal. Chem.*, 2016, **760**, 42-47.
12. R. Gulaboski and V. Mirceski, *Electrochim. Acta*, 2015, **167**, 219-225.
13. E. S. Rountree, B. D. McCarthy, T. T. Eisenhart and J. L. Dempsey, *Inorg. Chem.*, 2014, **53**, 9983-10002.
14. R. Kumar, H. Goel, S. K. Jha and R. Kant, *J. Electroanal. Chem.*, 2022, **905**, 115899.
15. J.-M. Noël and F. Kanoufi, *Curr. Opin. Electrochem.*, 2022, **35**, 101071.
16. S. Cannan, J. Cervera, R. J. Steliaros, E. Bitziou, A. L. Whitworth and P. R. Unwin, *Phys. Chem. Chem. Phys.*, 2011, **13**, 5403-5412.
17. R. Calhoun and A. Bard, *ECS Trans.*, 2011, **35**, 39-51.
18. T. J. Stockmann, J. M. Noël, S. Ristori, C. Combellas, A. Abou-Hassan, F. Rossi and F. Kanoufi, *Anal. Chem.*, 2015, **87**, 9621-9630.
19. T. Kai, M. Zhou, S. Johnson, H. S. Ahn and A. J. Bard, *J. Am. Chem. Soc.*, 2018, **140**, 16178-16183.
20. F. Kanoufi, C. Cannes, Y. Zu and A. J. Bard, *The Journal of Physical Chemistry B*, 2001, **105**, 8951-8962.
21. K. Barman, X. Wang, R. Jia and M. V. Mirkin, *J. Am. Chem. Soc.*, 2021, **143**, 8547-8551.
22. A. I. Romo, D. S. Abreu, F. P. T. de, M. S. Carepo, E. H. Sousa, L. Lemus, C. Aliaga, A. A. Batista, O. R. Nascimento, H. D. Abruna and I. C. Diogenes, *Chemistry*, 2016, **22**, 10081-10089.
23. D. Zigah, J. Rodríguez-López and A. J. Bard, *Phys. Chem. Chem. Phys.*, 2012, **14**, 12764-12772.
24. H. S. Park, K. C. Leonard and A. J. Bard, *The Journal of Physical Chemistry C*, 2013, **117**, 12093-12102.
25. H. S. Ahn and A. J. Bard, *J. Am. Chem. Soc.*, 2016, **138**, 313-318.
26. M. J. Counihan, W. Setwipatanachai and J. Rodríguez-López, 2019, **6**, 3507-3515.
27. Z. Jin and A. J. Bard, 2021, **60**, 794-799.

28. J. Rodríguez-López, M. A. Alpuche-Avilés and A. J. Bard, *J. Am. Chem. Soc.*, 2008, **130**, 16985-16995.
29. I. López, M. Cesbron, E. Levillain and T. Breton, *ChemElectroChem*, 2018, **5**, 1197-1202.
30. I. López, S. Dabos-Seignon and T. Breton, *Langmuir*, 2019, **35**, 11048-11055.
31. T. Breton and C. Gautier, in *Aryl Diazonium Salts and Related Compounds: Surface Chemistry and Applications*, eds. M. M. Chehimi, J. Pinson and F. Mousli, Springer International Publishing, Cham, 2022, pp. 97-120.
32. P. Hapiot, C. Lagrost and Y. R. Leroux, *Curr. Opin. Electrochem.*, 2018, **7**, 103-108.
33. D. Bélanger and J. Pinson, *Chem. Soc. Rev.*, 2011, **40**, 3995-4048.
34. C. Combellas, D.-e. Jiang, F. Kanoufi, J. Pinson and F. I. Podvorica, *Langmuir*, 2009, **25**, 286-293.
35. Y. R. Leroux, H. Fei, J.-M. Noël, C. Roux and P. Hapiot, *J. Am. Chem. Soc.*, 2010, **132**, 14039-14041.
36. K. Malmos, M. Dong, S. Pillai, P. Kingshott, F. Besenbacher, S. U. Pedersen and K. Daasbjerg, *J. Am. Chem. Soc.*, 2009, **131**, 4928-4936.
37. J. Billon, V. Shkirskiy, S. Dabos-Seignon, T. Breton and C. Gautier, *Phys. Chem. Chem. Phys.*, 2022, **24**, 14294-14298.
38. L. Pichereau, L. Fillaud, N. Kostopoulos, E. Maisonhaute, T. Cauchy, M. Allain, J.-M. Noël, C. Gautier and T. Breton, *J. Phys. Chem. Lett.*, 13, 2022, 11866-11871.
39. L. Pichereau, I. Lopez, M. Cesbron, S. Dabos-Seignon, C. Gautier and T. Breton, *Chem. Commun.*, 2019, **55**, 455-457.
40. T. Menanteau, E. Levillain, A. J. Downard and T. Breton, *Phys. Chem. Chem. Phys.*, 2015, **17**, 13137-13142.
41. T. Menanteau, E. Levillain and T. Breton, *Chem. Mater.*, 2013, **25**, 2905-2909.
42. A. J. Bard and M. V. Mirkin, *Scanning Electrochemical Microscopy*, Boca Raton, 2022.
43. D. Polcari, P. Dauphin-Ducharme and J. Mauzeroll, *Chem. Rev.*, 2016, **116**, 13234-13278.
44. J. Zhang, C. J. Slevin, C. Morton, P. Scott, D. J. Walton and P. R. Unwin, *The Journal of Physical Chemistry B*, 2001, **105**, 11120-11130.
45. M. T. Huynh, C. W. Anson, A. C. Cavell, S. S. Stahl and S. Hammes-Schiffer, *J. Am. Chem. Soc.*, 2016, **138**, 15903-15910.
46. P. P. Romańczyk, G. Rotko and S. S. Kurek, *Electrochem. Commun.*, 2014, **48**, 21-23.
47. C. Galli, *Chem. Rev.*, 1988, **88**, 765-792.
48. K. Daasbjerg and K. Sehested, *The Journal of Physical Chemistry A*, 2002, **106**, 11098-11106.
49. V. Shkirskiy, J. Billon, E. Levillain and C. Gautier, *Langmuir*, 2021, **37**, 12834-12841.
50. J. S. Barroso-Martínez, A. I. B. Romo, S. Pudar, S. T. Putnam, E. Bustos and J. Rodríguez-López, *J. Am. Chem. Soc.*, 2022, **144**, 18896-18907.